Macromolecular Rapid Communications
www.mrc-journal.de

Nonlinear Influence of Blending Star and Triblock Copolymers on Morphological and Mechanical Properties of Thermoplastic Elastomers

*Max G. Schußmann, Leonardo Rocha Dias, Simon Buchheiser, Hermann Nirschl, Jonathan Berson, Manfred Wilhelm, and Valerian Hirschberg**

To tune the mechanical properties of thermoplastic elastomers, a linear Poly(styrene (S)-*b*-isoprene (I)-*b*-styrene (S)) triblock copolymer (SIS) is blended with well-defined symmetric star-shaped PS-PI block copolymers with 8 and 15 arms, respectively. The model systems are synthesized via anionic polymerization and grafting-onto techniques and have a lamellar morphology with the long-range order L_0 for the SIS larger than the stars. Morphological analysis using small angle X-ray scattering (SAXS) and atom force microscopy (AFM) reveals a nonlinear dependency of L_0 as a function of the star content, ϕ_{star}. For small star contents, L_0 of the blends increases above L_0 of the individual compounds. The stars show significantly higher mechanical performance than the SIS, by an increased elongation at break, ϵ_b, by +15% and +38%, and an increased ultimate tensile strength, σ_{UTS}, by about a factor of 2. For the blends, the mechanical properties highly depend on the star content, and can be fully uncoupled from the ones of the SIS and the star: at small star contents ϵ_b is significantly improved beyond $\epsilon_{b,star}$, but σ_{UTS} decreases below $\sigma_{UTS,SIS}$. For higher star contents, σ_{UTS} strongly increases toward $\sigma_{UTS,star}$, whereas ϵ_b shows a minimum around $\phi_{star} = 50$ wt.%, before increasing to $\epsilon_{b,star}$.

1. Introduction

Modifications of polymers have been done since the 1920s by first simple physical blending polystyrene (PS) with a rubbery material to improve mechanical properties.[1] Today thermoplastic elastomers (TPE), i.e., materials with rubber-like elasticity at lower temperatures but thermoplastic-like processability at higher temperatures are made of block copolymers.[2] To generate the mechanical strength of the TPE, phase separation of block copolymers enables the replacement of chemical crosslinking in rubber by physical crosslinking. Commonly linear ABA triblock copolymers are used with a hard block A (high glass transition temperature T_g) and a rubbery block B (low T_g), i.e., the application temperature of the TPE is below the T_g of the block A, but above the T_g of the block B.[3]

The phase separation is driven by the repulsion of, unlike polymer segments. The segregation strength in the simple case of block copolymers is described by the product $N\chi$, where χ is the Flory–Huggins interaction parameter, which decreases ≈1/T, and N is the total degree of polymerization. In a diblock copolymer consisting of two building blocks A and B, the volume composition can be described as

$$f_A = \frac{N_A \rho_A}{N_A \rho_A + N_B \rho_B} \tag{1}$$

where N is the number of monomers per block, f is the volume fraction of the corresponding monomer and ρ is the respective density. The order–disorder transition, ODT, takes place when

M. G. Schußmann, L. R. Dias, M. Wilhelm, V. Hirschberg
Institute for Chemical Technology and Polymer Chemistry
Karlsruhe Institute of Technology (KIT)
Engesserstraße 18, 76131 Karlsruhe, Germany
E-mail: valerian.hirschberg@kit.edu

S. Buchheiser, H. Nirschl
Institute of Mechanical Process Engineering and Mechanics
Karlsruhe Institute of Technology (KIT)
Am Forum 8, 76131 Karlsruhe, Germany

J. Berson
Institute of Nanotechnology
Karlsruhe Institute of Technology (KIT)
Am Forum 8, 76131 Karlsruhe, Germany

V. Hirschberg
Institute for Technical Chemistry
Technical University Clausthal
Arnold-Sommerfeld-Str. 4, 38678 Clausthal-Zellerfeld, Germany

The ORCID identification number(s) for the author(s) of this article can be found under https://doi.org/10.1002/marc.202500131

DOI: 10.1002/marc.202500131

Table 1. Overview of the molecular, morphological, and mechanical properties of the linear SIS triblock and stars with SI diblock arms used for the blends.

	$M_{w,arm}$ [kg mol^{-1}]	$M_{w,t}$ [kg mol^{-1}]	Arm number q	$Đ_t$	ϕ_{PS} [vol%]	Bulk Morphology	L_0 [nm]	σ_{UTS} [MPa]	ϵ_b [%]
SIS	–	129	2	1.07	32	L	47.2	9.9 ± 1.5	862 ± 25
$(SI)_8$	55	423	8	1.11	28.5	L	29.7	21 ± 3.8	971 ± 58
$(SI)_{15}$	52	788	15	1.08	26	L	32.7	20.8 ± 0.8	1106 ± 36

$N\chi$ reaches a critical value either by adjusting the total molecular weight of the polymer or by temperature change. The minimum $N\chi$ for phase separation to occur is typically at $N\chi = 10$ for linear diblock and $f_A = f_B = 0.5$[4] or $N\chi = 18$ for symmetric ABA triblock copolymers.[2,5] In this case self-assembly leads to a lamellar structure for linear diblock copolymers. For $f_A > 1/2$, respectively $f_B > 1/2$, the morphology results in a cylindrical or spherical structure due to interfacial curvature driven by surface tension.[6–8]

For TPEs, a morphology with a continuous soft matrix B with a spherical or hexagonal cylindrical microstructure of A is commonly targeted. For PS–PI block copolymers, χ is at room temperature ≈0.1, requiring therefore N >> 100 for phase separation.[9] To avoid a lamellar morphology, less than 35 vol % of the rigid PS component can be copolymerized according to the typical phase diagrams for di- and triblock copolymers.[8]

To improve the mechanical properties of TPEs beyond those of linear ABA triblock copolymers,[10] more complex topologies have been investigated including multiblock copolymers,[11–13] linear low disperse SIS triblock with different shapes of the MWD of the first S block,[14–16] asymmetric triblocks[17] or branched block copolymers with a (miktoarm) star,[17] branched comb-like multigraft copolymers (MGCs)[18,19] and pom-pom[20] architectures. It has been shown that branched topologies allow the uncoupling of the volume fraction–morphology relationship of ABA triblock copolymers and enables a significant improvement in the mechanical properties, especially with respect to ultimate tensile stress, σ_{UTS}, and elongation at break, ϵ_b.

Whereas ABC terpolymers allow the access of even new morphologies,[21] another elegant method to tune morphologies, induce order-to-order transitions, and enhance mechanical properties of block copolymers is by blending homo- and/or block copolymers of different block length, block number, block order or topology.[22–29] Blending an asymmetric ABA triblock copolymer with linear PS homopolymer (hPS) led to a lamellar to hexagonal to lamellar order–order transition with increasing volume fraction of hPS.[25] For the blends of a linear PS with a PS/PI miktoarm star, unexpected continuous PI phases could be obtained even at high ϕ_{PS}: For a blend with 82 wt.% PS, a new morphology with a continuous PI phase was found, described as a "bricks and mortar mesophase."[30] This resulted in a stiff TPE with high elasticity and high elongation at break. For a blend with ϕ_{PS} = 97 vol% of PS-PI mictoarm star with hPS, even a lamellar morphology was obtained.[31]

Tapered SI diblock blended with $(SI)_n$ multiblock copolymers with different block numbers and molecular weights of the blocks allowed to substantial increase the mechanical properties of the SI diblock.[32] Blends with large differences in the long-range order L_0 between tapered $(SI)_5$ and tapered SI of over ΔL_0 = 15 nm started to be partially immiscible, with full immiscibility for $\Delta L_0 > 47$ nm, i.e., many small domains of the $(SI)_5$ appeared to be immiscible with SI containing large domains, which resulted in a decrease in mechanical performance. For the miscible blends, a nearly linear dependency of the domain spacing as a function of the $(SI)_3$ weight content was found, combined with a ≈50-fold increase of the elongation at break for a 50 wt.% blend of SI/$(SI)_3$ compared to the neat SI. This could be explained by a bridging of the micro domain via the multiblock copolymers.

In ABA triblock copolymers, the outer A blocks can be located in either the same domain, so that B dorms a so-called loop, or in two different domains, so B forms a bridge between the two A domains. Domain bridging is associated with increased mechanical performance compared to loops. For SIS triblock copolymers with a lamellar morphology, only ≈41% of the PI blocks were found to bridge,[33,34] whereas in stars with SI arms (S outer, I inner block) and with 9 or more arms nearly all PI blocks are predicted to bridge.[35]

The objective of this article is to investigate the morphological and mechanical properties of blends of linear SIS triblock copolymer and two $(SI)_n$ stars with 8 and 15 arms, respectively, similar ϕ_{PS}, lamellar morphology, and full miscibility. The two $(SI)_n$ stars have significantly higher ultimate tensile stress and elongation at break than the linear SIS, so the question is how the mechanical properties of the SIS can be tuned and improved by the addition of the star-shaped block copolymers. The results show a nonlinear behavior for the morphological domain size of the blends with an unexpected increase of L_0 above L_0 of the SIS and the star for small star fractions and a drastic increase in mechanical properties with the addition of even 10 wt.% of $(SI)_n$.

2. Results and Discussion

2.1. Materials and Methods

The stars $(SI)_8$ and $(SI)_{15}$ were synthesized as described previously.[36] The SIS triblock copolymer was synthesized by sequential monomer addition (styrene, isoprene, styrene), initiated by *s*-BuLi in cyclohexane as described previously.[10] Molecular weights were determined by SEC-MALLS using for dn/dc the weighted average composition as determined by ^{1}H NMR spectroscopy with 0.187 mL g^{-1} for PS and 0.111 mL g^{-1} for PI.[20,37] The molecular characteristics of the stars and the SIS are listed in **Table 1**.

Blends were prepared by dissolution in THF and stirring overnight. The solution was cast into an aluminum dish and the solvent evaporated slowly over 4 days. Afterward, the films were annealed under vacuum at 120 °C for 4 h. Specimens for SAXS

Figure 1. The blends investigated herein are made of a) triblock and 15-arm star and b) triblock and 8-arm star.

and tensile measurements were cut from the films. Both blend systems are schematically shown in **Figure 1**.

Stress–strain curves were measured on a Hegewald–Peschke inspect table 10 kN in uniaxial testing at a linear strain rate of $\epsilon = 0.0833\ s^{-1}$ with dog bone specimens (DIN 53 504) at room temperature. Small-angle X-ray scattering was conducted on a Xeuss 2.0 Q-Xoom, Xenocs SA, Grenoble, France, $q = 0.001 - 4\ nm^{-1}$. Atomic force microscopy (AFM) was done in semicontact mode using a Bruker dimension ICON system equipped with an Opus 160AC-NA by Mikromasch tip (typical force constant 26 N m^{-1}). The AFM samples were prepared on silicon wafers freshly cleaned by snowjet by spin-coating at 5000 rpm of 0.3 wt.% solutions in toluene, yielding films with a thickness of 15 ± 1 nm.

2.2. Morphological Characterization

To investigate the morphology of the block copolymers and their blends, SAXS and AFM experiments were performed. The SIS and the $(SI)_n$ stars have similar ϕ_{PS} (see Table 1) and as shown by the SAXS and AFM analysis from **Figures 2** and **3** a lamellar morphology. The SAXS patterns show scattering peaks at q_0, $2q_0$, $3q_0$, etc., indicating a strong phase separation and a very good long-range order. SAXS and AFM indicate good miscibility between the linear SIS and the stars. The investigated stars have larger q_0, i.e., smaller long-range-order distances L_0, than the SIS with a difference in L_0 of $\Delta L_0 = 14.5$ nm and 17.5 nm for the 15- and the 8-arm star, respectively.

For the blends of the SIS with the $(SI)_{15}$ in Figure 2a), q_0 first decreases below $q_{0,SIS}$ for $(SI)_{15}$ fractions less than 20 wt.% and then increases to the q_0 of the $(SI)_{15}$. A similar trend is observed for the $(SI)_8$ blends and the higher order peaks at $2q_0$ and $3q_0$, still indicating a lamellar morphology for all blends. The clearly nonlinear behavior of L_0 as a function of ϕ_{Star} for the SIS/$(SI)_n$ blends is also in contrast to the observed behavior of miscible blends of tapered SI and SISISI di- and multiblock copolymers, which displayed a nearly linear behavior in the domain spacing with increasing blend content.[32]

Furthermore, the AFM analysis reveals striking differences between the neat SIS and the SIS/$(SI)_n$ blends: compared with the neat SIS the addition of 5 wt.% $(SI)_{15}$ in Figure 3b) not only results in larger domain spacing L_0 but also in larger areas of the PS domain. Instead of many small PS domains for the SIS, fewer but larger PS areas can be identified for the SIS/$(SI)_{15}$-5%. This is also observed for the higher $(SI)_{15}$ weight content, but with again smaller L_0.

2.3. Mechanical Testing

The stress-strain curves of the neat SIS, $(SI)_{15}$, $(SI)_8$, and the blends are shown in **Figure 4** with a zoom for small strains. First, the neat $(SI)_{15}$ and $(SI)_8$ clearly outperform the SIS in terms of ultimate tensile stress σ_{UTS} by about a factor of 2 and reach for both stars around $\sigma_{UTS} = 21$ MPa, which is within the benchmark value for most PS/PI block copolymer model systems, as described in literature overview recently.[20] The increase in mechanical performance is also expected from the increase in domain bridging for a star with a high arm number, compared to linear SIS.[33–35] The elongation of break is increased by ≈20% from $\epsilon_b = 860 \pm 25\%$ for the SIS to about $\epsilon_b > 1000\%$ for the stars. As shown in Figure 4a,b, the neat stars clearly show yielding, which is less pronounced for the SIS.

It is important to note, that tensile tests could not be performed for the blend with 3 wt.% $(SI)_8$ in the SIS, since the material was too brittle and the specimen broke during preparation. The mechanical analysis of the blends reveals, that different blend ratios allow tuning the mechanical properties beyond those of the SIS and that the simple expectation of linear addition of the properties of the SIS and the stars do not hold: For the SIS/$(SI)_{15}$ blends with only 5 wt.% of $(SI)_{15}$, the material becomes very soft with an increase of $\epsilon_b = 860 \pm 25\%$ for the SIS to $\epsilon_b = 1050 \pm 71\%$ for the SIS/5%$(SI)_{15}$ blend, but a reduction of σ_{UTS} by a factor of 2 and 4, compared to the neat SIS and $(SI)_8$, respectively. In contrast, the addition of 10 and 20 wt.% of $(SI)_{15}$ to the SIS resulted in a drastic increase in ϵ_b beyond those of the SIS and σ_{UTS} nearly increases to the high level of the $(SI)_{15}$. A similar trend was found for the blends with the $(SI)_8$ in Figure 4b).

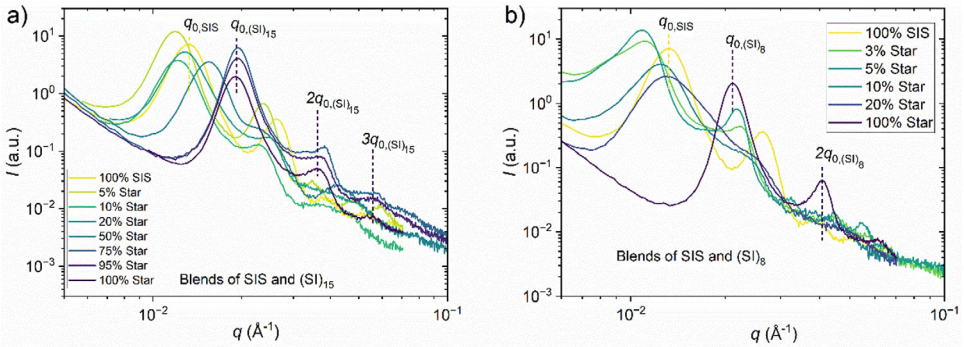

Figure 2. Azimuthally-averaged SAXS scattering of the blends of the triblock with a) 15-arm star and b) 8-arm star. The q_0 scattering peaks of neat SIS and star are indicated. For small ϕ_{star}, the q_0 maximum is even shifted to q-values smaller than the neat polymers.

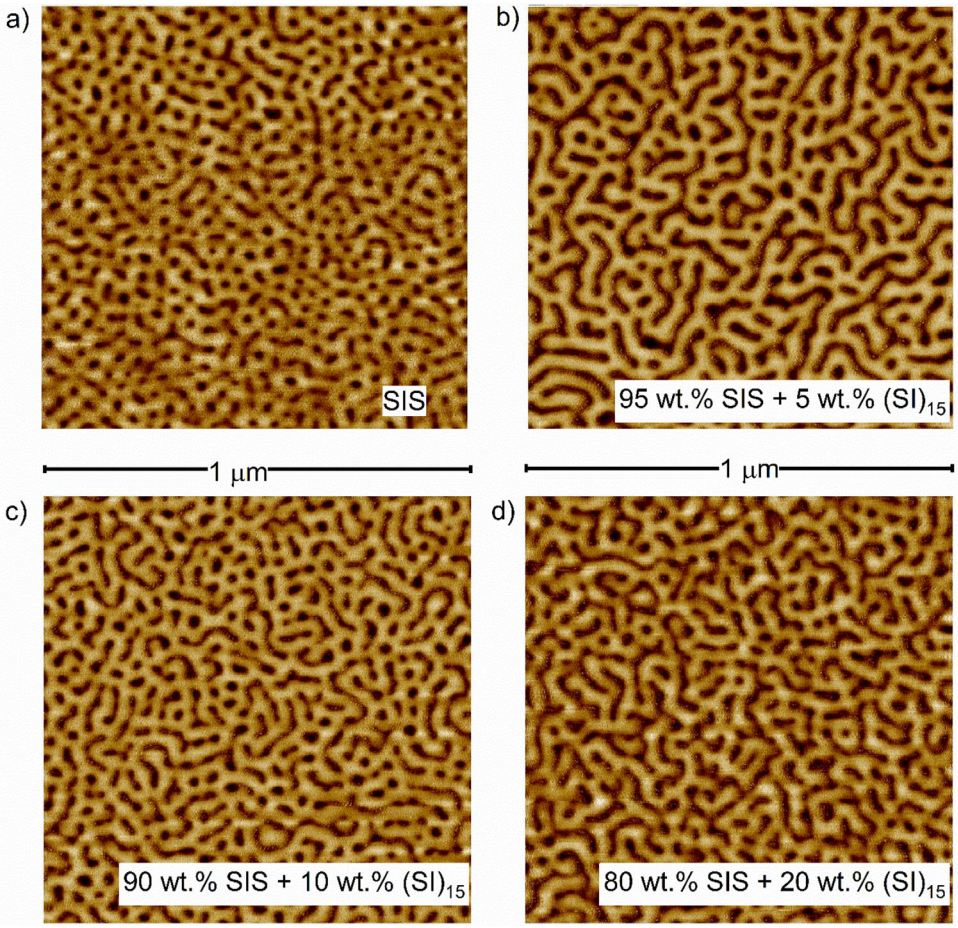

Figure 3. AFM images of the neat SIS and of blends with 5, 10, and 20 wt.% $(SI)_{15}$. The differences between the neat SIS and the blends can be seen clearly as the domain spacing increases. For the blends, the size, or rather the continuous area of the PS domains increases drastically.

2.4. Morphology–Mechanical Property Relationship

To establish structure-property relationships, mechanical key parameters have been analyzed as a function of the star volume fraction ϕ_{star} together with L_0: in **Figure 5** the ultimate tensile stress, in **Figure 6** the elongation at break, and in **Figure 7** the Young's E modulus. Whereas both stars have higher σ_{UTS}, $\epsilon_{b,}$ and Young's modulus, but a smaller L_0 than the SIS, the trend for the blends is not simply linear between the properties of the SIS and the stars.

In Figure 5a for the SIS/$(SI)_{15}$ blends, σ_{UTS} first decreases at ϕ_{star} = 5 and 10 wt.% when L_0 also increases to L_0 = 52.8 nm, i.e., beyond $L_{0,(SI)15}$ = 32.7 nm and $L_{0,SIS}$ = 47.2 nm. For ϕ_{star} > 10 wt.%, σ_{UTS} increases rapidly toward the σ_{UTS} of the star, with also L_0 decreasing below L_0 of the SIS and reaching around ϕ_{star} > 75 wt.% the L_0 value of the star. For the SIS/$(SI)_8$ blends a similar trend is found at low ϕ_{star}, where σ_{UTS} decreases below σ_{UTS} of the star and correlates with an increased L_0.

In contrast to σ_{UTS}, as shown in Figure 6a), ϵ_b increases drastically at low ϕ_{star}. For the SIS/$(SI)_{15}$ blends, the addition of 5 wt.% $(SI)_{15}$ to the SIS results in an increase from ϵ_b = 860 ± 25% to ϵ_b = 1050 ± 71%. With increasing star content, ϵ_b first decreases again until it reaches around ϕ_{star} = 50 wt.% a similar ϵ_b as the SIS, and then increases rapidly toward the ϵ_b of the neat $(SI)_{15}$. For the $(SI)_8$ a similar trend is observed at ϕ_{star} < 20 wt.%, with a drastic increase in ϵ_b when also L_0 increases above the L_0 of the SIS. The Young's modulus is shown in Figure 7a) for the SIS/$(SI)_{15}$ blends, revealing also an unexpected trend at low ϕ_{star}. For ϕ_{star} < 20 wt.%, the Young's modulus decreases compared to the Young's modulus of the SIS by up to about a factor of three, i.e., the material gets significantly softer, as also indicated by ϵ_b. For ϕ_{star} > 20 wt.%, Young's modulus increases until it finally reaches the value of the neat star. For the SIS/$(SI)_8$ blends, a similar trend for Young's modulus as a function of ϕ_{star} is found.

For ϕ_{star} < 20 wt.%, the softening of the material quantified by increased ϵ_b but drastically decreased σ_{UTS} and E as well as the increased L_0 indicates reduced domain bridging on the molecular level and increased domain looping of the block copolymer chains. In contrast, it indicates that at high ϕ_{star} domain bridging is significantly increased compared to domain looping for the pure SIS, as predicted by self-consistent field theory.[33,35]

The analysis of the mechanical properties (σ_{UTS}, ϵ_b and Young's E modulus) as a function of ϕ_{star} reveals a complex structure-property relationship and blending of a SIS and a star-shaped SI block copolymer allows to tune the material properties

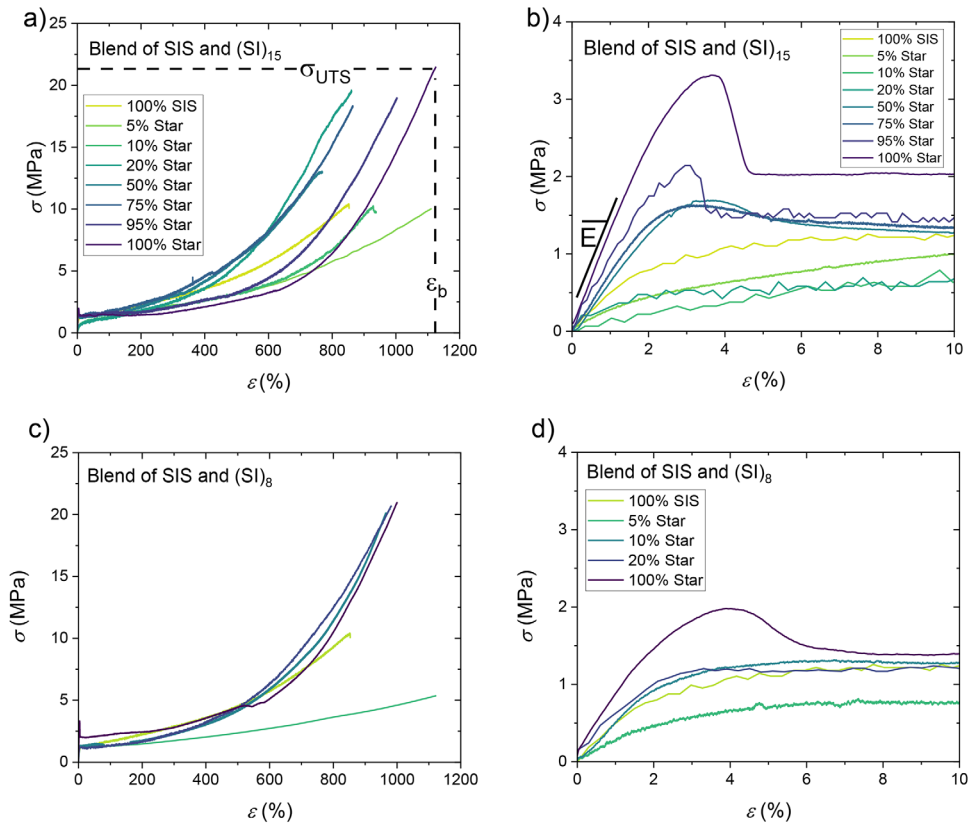

Figure 4. Stress–strain curves of the blends of linear triblock with a) 15 arm star, b) the zoom-in to small strains, c) 8 arm star, and d) again the zoom-in to small strains. Tensile tests were conducted at a crosshead speed of 5 mm s^{-1}, which corresponds to a linear strain rate of $\dot{\epsilon} = 0.0083\ s^{-1}$.

beyond the one of the SIS and the star. In particular the unexpected morphological and mechanical behavior of the blends having $\phi_{star} < 20$ wt.% is striking. The addition of $\phi_{star} < 20$ wt.% leads to an increase in L_0 beyond those of the SIS and the star, which highly impacts the mechanical properties and leads to a softer material than its individual blend components with lower Young's modulus and ultimate tensile stress, but therefore a significantly increased elongation at break. At $\phi_{star} > 20$ wt.%, the ultimate tensile stress increases drastically compared to the SIS, whereas ϵ_b and E have similar values as the SIS and then increase further to one of the neat stars. The blending of the linear SIS and the $(SI)_n$ consequently allows to fully uncouple L_0, σ_{UTS}, ϵ_b, and Young's modulus and tunes the desired mechanical properties.

3. Conclusion

To tune the mechanical properties of thermoplastic elastomers, a linear Polystyrene (PS)-polyisoprene (PI)-polystyrene (PS) triblock copolymer (SIS) is blended with well-defined star-shaped PS-PI block copolymers with 8 and 15 arms, respectively. The low-disperse model systems have a PS content ≈30 vol% and were synthesized via anionic polymerization and grafting-onto

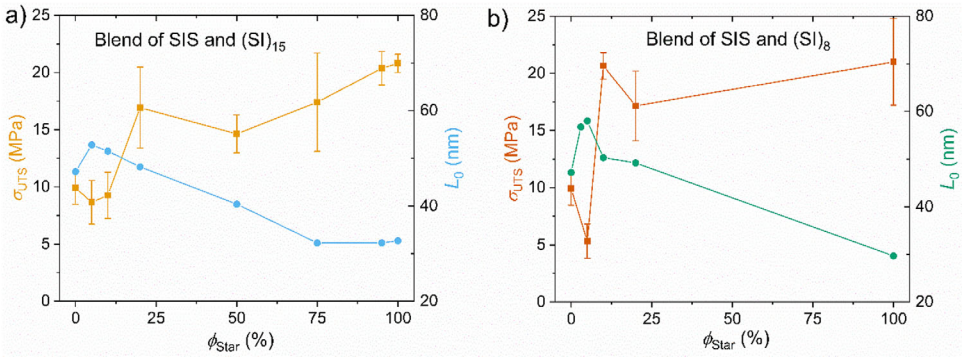

Figure 5. Ultimate tensile strength σ_{UTS} of the blends of the SIS with a) the 15-arm star and b) the 8-arm star as a function of the star volume fraction on the left *y*-axis and the domain size L_0 on the right *y*-axis.

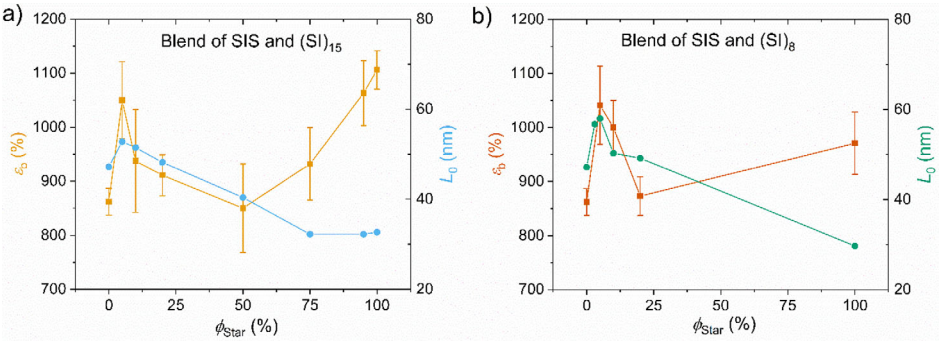

Figure 6. Strain at break ϵ_b of the blends of the SIS with a) the 15-arm star and b) the 8-arm star as a function of the star volume fraction on the left y-axis and the domain size L_0 on the right y-axis. At $\phi_{star} < 10$ wt.%, L_0 increases beyond L_0 of both, SIS and star, and the elongation at break increases drastically compared with the neat SIS.

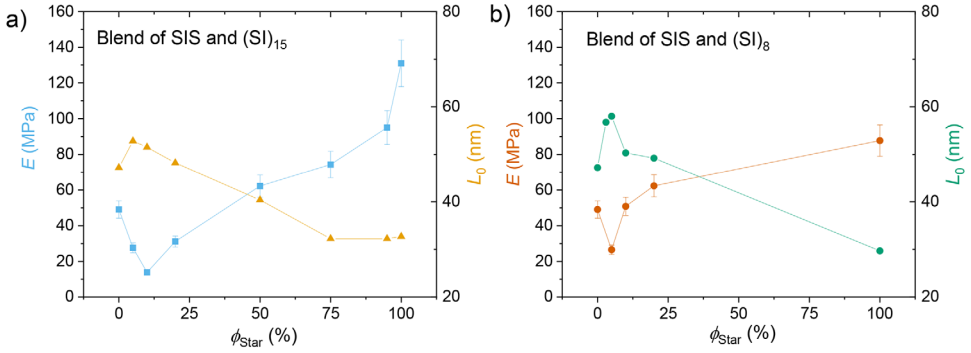

Figure 7. Young's-Modulus E of the blends of the SIS with a) the 15-arm star and b) the 8-arm star as a function of the star volume fraction on the left y-axis and the domain size L_0 on the right y-axis. Similar to ϵ_b, at $\phi_{star} < 10$ wt.%, also Young's modulus decreases drastically below E of the SIS and the star, indicating a softening of the blend.

techniques. The SIS and the stars have a lamellar morphology with the long-range order L_0 for the SIS larger than the stars and are fully miscible with each other as shown by the morphological analysis done with small angle X-ray scattering (SAXS) and atom force microscopy (AFM). The results reveal a nonlinear trend of L_0 as a function of the star content, ϕ_{star}, with an unexpected increase of L_0 above L_0 of the SIS and stars for small star contents. The stars have a significantly higher mechanical performance than the SIS, by an increased elongation at break, ϵ_b, by +15% and +38%, and ultimate tensile strength, σ_{UTS}, by about a factor of 2. For the blends, the morphological and mechanical properties highly depend on the star content, and can be fully uncoupled from the ones of the SIS and the star: at small star content, L_0 of the blends is larger than L_0 of the SIS or the stars and ϵ_b significantly increases beyond $\epsilon_{b,star}$, but σ_{UTS} decreases below $\sigma_{UTS,SIS}$, indicating reduced domain bridging. For higher star contents, σ_{UTS} strongly increases toward $\sigma_{UTS,star,}$ whereas ϵ_b shows a minimum around $\phi_{star} = 50$ wt.%, before increasing to $\epsilon_{b,star}$. This shows the potential to fully uncouple and tune morphological and mechanical properties from molecular characteristics and the PS/PI volume fraction by blending block copolymers of different complex architectures.

Future dielectric spectroscopic investigations of the domain bridging/looping of complex block copolymer blends would be of great interest.

Acknowledgements

V.H. acknowledges funding from the German Research Foundation (DFG grant number, HI 2467/1-1, #529315409). The authors thank Michael Pollard for proofreading the manuscript as a native English speaker.

Open access funding enabled and organized by Projekt DEAL.

Conflict of Interest

The authors declare no conflict of interest.

Data Availability Statement

The data that support the findings of this study are available from the corresponding author upon reasonable request.

Keywords

blends, block copolymers, complex topologies, mechanical properties, phase separation

Received: February 7, 2025
Revised: April 8, 2025
Published online:

[1] *Applied Polymer Science: 21st Century*, 1st ed., (Eds: C. Craver, C. Carraher), Elsevier Science & Technology, Oxford, New York **2000**.
[2] I. W. Hamley, *The Physics of Block Copolymers*, Oxford Science Publications; Oxford University Press, Oxford, New York **1998**.
[3] W. Wang, W. Lu, A. Goodwin, H. Wang, P. Yin, N.-G. Kang, K. Hong, J. W. Mays, *Prog. Polym. Sci.* **2019**, *95*, 1.
[4] A. K. Khandpur, S. Foerster, F. S. Bates, I. W. Hamley, A. J. Ryan, W. Bras, K. Almdal, K. Mortensen, *Macromolecules* **1995**, *28*, 8796.
[5] B. Abu-Sharkh, A. AlSunaidi, *Macromol. Theory Simul.* **2006**, *15*, 507.
[6] F. S. Bates, M. A. Hillmyer, T. P. Lodge, C. M. Bates, K. T. Delaney, G. H. Fredrickson, *Science* **2012**, *336*, 434.
[7] F. S. Bates, *Science* **1991**, *251*, 898.
[8] F. S. Bates, G. H. Fredrickson, *Phys. Today* **1999**, *52*, 32.
[9] J. N. Owens, I. S. Gancarz, J. T. Koberstein, T. P. Russell, *Macromolecules* **1989**, *22*, 3380.
[10] V. Hirschberg, L. Faust, D. Rodrigue, M. Wilhelm, *Macromolecules* **2020**, *53*, 5572.
[11] R. D. Barent, I. Perevyazko, N. Mikusheva, G. Floudas, H. Frey, *Macromolecules* **2023**, *56*, 5792.
[12] M. Heck, C. Botha, M. Wilhelm, V. Hirschberg, *Macromol. Rapid Commun.* **2021**, *42*, 2100448.
[13] M. Steube, T. Johann, E. Galanos, M. Appold, C. Rüttiger, M. Mezger, M. Gallei, A. H. E. Müller, G. Floudas, H. Frey, *Macromolecules* **2018**, *51*, 10246.
[14] S. I. Rosenbloom, J. H. Hsu, B. P. Fors, *J. Polym. Sci.* **2022**, *60*, 1291.
[15] S. I. Rosenbloom, D. T. Gentekos, M. N. Silberstein, B. P. Fors, *Chem. Sci.* **2020**, *11*, 1361.
[16] S. I. Rosenbloom, B. P. Fors, *Macromolecules* **2020**, *53*, 7479.
[17] W. Shi, N. A. Lynd, D. Montarnal, Y. Luo, G. H. Fredrickson, E. J. Kramer, C. Ntaras, A. Avgeropoulos, A. Hexemer, *Macromolecules* **2014**, *47*, 2037.
[18] Y. Zhu, E. Burgaz, S. P. Gido, U. Staudinger, R. Weidisch, D. Uhrig, J. W. Mays, *Macromolecules* **2006**, *39*, 4428.
[19] R. Weidisch, S. P. Gido, D. Uhrig, H. Iatrou, J. Mays, N. Hadjichristidis, *Macromolecules* **2001**, *34*, 6333.
[20] V. Hirschberg, M. G. Schußmann, M.-C. Röpert, N. Dingenouts, S. Buchheiser, H. Nirschl, J. Berson, M. Wilhelm, *Macromolecules* **2024**, *57*, 3387.
[21] C. Auschra, R. Stadler, *Macromolecules* **1993**, *26*, 2171.
[22] G. S. Doerk, K. G. Yager, *ACS Nano* **2017**, *11*, 12326.
[23] A. J. Mueller, A. P. Lindsay, A. Jayaraman, T. P. Lodge, M. K. Mahanthappa, F. S. Bates, *ACS Macro Lett.* **2020**, *9*, 576.
[24] Z. Shen, K. Luo, S. J. Park, D. Li, M. K. Mahanthappa, F. S. Bates, K. D. Dorfman, T. P. Lodge, J. I. Siepmann, *JACS Au* **2022**, *2*, 1405.
[25] W. Shi, W. Li, K. T. Delaney, G. H. Fredrickson, E. J. Kramer, C. Ntaras, A. Avgeropoulos, N. A. Lynd, *J. Polym. Sci. Part B Polym. Phys.* **2016**, *54*, 169.
[26] B. Zhang, S. Cui, T. P. Lodge, F. S. Bates, *Macromolecules* **2023**, *56*, 1663.
[27] A. P. Lindsay, G. K. Cheong, A. J. Peterson, S. Weigand, K. D. Dorfman, T. P. Lodge, F. S. Bates, *Macromolecules* **2021**, *54*, 7088.
[28] R. Adhikari, M. Buschnakowski, W. Lebek, R. Godehardt, G. H. Michler, F. J. B. Calleja, K. Knoll, *Polym. Adv. Technol.* **2005**, *16*, 175.
[29] R. Lach, R. Weidisch, A. Janke, K. Knoll, *Macromol. Rapid Commun.* **2004**, *25*, 2019.
[30] W. Shi, A. L. Hamilton, K. T. Delaney, G. H. Fredrickson, E. J. Kramer, C. Ntaras, A. Avgeropoulos, N. A. Lynd, Q. Demassieux, C. Creton, *Macromolecules* **2015**, *48*, 5378.
[31] W. Shi, A. L. Hamilton, K. T. Delaney, G. H. Fredrickson, E. J. Kramer, C. Ntaras, A. Avgeropoulos, N. A. Lynd, *J. Am. Chem. Soc.* **2015**, *137*, 6160.
[32] M. Steube, M. Plank, M. Gallei, H. Frey, G. Floudas, *Macromol. Chem. Phys.* **2021**, *222*, 2000373.
[33] H. Watanabe, H. Tan, *Macromolecules* **2004**, *37*, 5118.
[34] H. Watanabe, *Macromolecules* **1995**, *28*, 5006.
[35] R. K. W. Spencer, M. W. Matsen, *Macromolecules* **2017**, *50*, 1681.
[36] M. G. Schußmann, L. Kreutzer, V. Hirschberg, *Macromol. Rapid Commun.* **2024**, *45*, 2300674.
[37] R. Velichkova, V. Toncheva, C. Getova, S. Pavlova, L. Dubrovina, E. Gladkova, M. Ponomareva, *J. Polym. Sci. Part Polym. Chem.* **1991**, *29*, 1107.